ANALYSIS OF ICRF ($\omega \leq \omega_{ci}$) PLASMA PRODUCTION IN LARGE SCALE TOKAMAKS

A.I. LYSOJVAN, V.E. MOISEENKO, O.M. SHVETS, K.N. STEPANOV
Institute of Physics and Technology,
Khar'kov, Ukraine

ABSTRACT. The paper studies the possibility of target plasma radiofrequency (RF) production in the ion cyclotron range of frequencies (ICRF) ($\omega \leq \omega_{ci}$) in large scale tokamaks before the startup of an Ohmic discharge. A number of experimental and theoretical studies on dense plasma production in the ICRF in toroidal magnetic devices are reviewed. The criteria for optimal development of the RF discharge stages are analysed, i.e. for RF breakdown of the neutral fill gas in the vicinity of the antenna (non-wave stage, $n_e \ll n_a$, where n_e and n_a are the densities of electrons and atoms), and the wave stages of initial ionization ($n_e < n_a$) and neutral gas burnout ($n_e \sim n_a$) in the whole volume of the plasma torus. A number of requirements for the design of the antenna system are formulated for all stages of dense plasma ICRF production. A scenario for plasma ICRF production with slot type antennas in the ITER tokamak is proposed. Numerical simulations with a 0-D transport code show that in ITER a target plasma with an electron density of $\approx 3 \times 10^{12}$ cm^{-3} can be produced by coupling 3-6 MW of RF power to the plasma at a frequency of ≈ 3 MHz. Such a level of RF power is sufficient not only for full ionization of the neutral gas but also for heating the produced plasma to electron temperatures of approximately 80 eV.

1. INTRODUCTION

There are a number of problems concerning the initial stage of Ohmic discharges in large scale tokamaks. One of these problems is the high loop voltage necessary to achieve Ohmic breakdown of the neutral fill gas and subsequent plasma production. This involves engineering difficulties connected with the inductor design [1]. Additionally, a beam of runaway electrons is produced by the high initial loop voltage, increasing the energy losses from the Ohmic discharge at the quasi-steady stage [2, 3].

Another problem concerns the large inductor magnetic flux losses at the Ohmic startup stage [4, 5], as a result of which the duration of the pulse is reduced. In addition to the above mentioned problems, there is the necessity of controlling the location at which the plasma column is formed and of reproducing the discharges.

One of the possible ways to solve these problems is to produce an initial plasma before the start of the Ohmic discharge [6, 7]. In this case, the Ohmic discharge begins in the current ramp-up stage, for which these problems are not of primary importance.

A number of experiments (see, for example, Refs [8–13]) shows that initial plasma production in tokamaks lowers the loop voltage considerably, decreases the expense of inductor magnetic flux, suppresses electron runaway, broadens the initial pressure range of the neutral gas and improves the reproducibility of the discharge.

Among the possible non-Ohmic techniques of plasma production, those using radiofrequency (RF) seem to be most promising. In recent years, preionization and plasma production techniques in the electron cyclotron (EC) [8–12, 14–16], lower hybrid (LH) [13, 17, 18] and ion cyclotron (IC) [19–32] ranges of frequencies have been developed intensively.

In this paper we present a study of the possibility of target plasma RF production in tokamaks (including large scale ones) in the ion cyclotron range of frequencies (ICRF). The increased interest in this range (1–60 MHz) is due to the availability of powerful quasi-steady RF sources ($P_{rf} \approx 20$ MW, $\tau_{rf} \approx 20$ s) of comparatively low cost [33] and also to the fact that plasma can be produced in a broad range of confining magnetic fields without the necessity of retuning the RF generator frequency [20, 25, 26, 32]. It has been shown that in the ICRF it is possible to produce plasma in open traps and toroidal magnetic devices by exciting fast magnetosonic (FMS) waves [25, 27, 28, 32, 34], IC waves [19–22, 24–32, 35–38] and Alfvén waves [19–26, 29, 32].

The paper is organized as follows. Section 2 gives a review of a number of experimental studies on plasma production using the ICRF technique on the OMEGA toroidal device without rotational transform [26, 29], the URAGAN-2 stellarator [20–22, 24], and the URAGAN-3 [25–27, 30, 31] and CHS [32] torsatrons. Section 3 contains a theoretical analysis of plasma production mechanisms with the ICRF technique in toroidal magnetic devices without rotational transform.

With the help of a 0-D transport model, calculations of the target plasma production process in an ITER type device at the neutral gas burnout and fully ionized plasma heating stages have been performed. It is proposed to use low impedance slot type antenna systems for RF power coupling to fusion scale devices. The studies on plasma ICRF production are summarized in Section 4.

2. EXPERIMENTS ON PLASMA RF PRODUCTION IN THE $\omega < \omega_{ci}$ FREQUENCY RANGE

2.1. Experiments on the OMEGA toroidal device

Plasma ICRF production has been studied in a number of experiments performed on the OMEGA device without rotational transform [26, 29] (major radius of the torus R = 44 cm, vessel radius r = 10 cm, plasma radius $\bar{a}$ = 7 cm, toroidal magnetic field $B_0 \leq 10$ kG and vertical magnetic field $B_\perp < 0.1$ kG). RF power ($P_{rf} \approx 200$ kW) has been coupled to the device by using electromagnetic antennas of either frame type [21, 26] or slot type [21, 22] without electrostatic shields.

The frame type antenna is a current carrying frame extended along the magnetic field lines in the toroidal direction and unprotected by a dielectric. Such an antenna was placed inside the vacuum vessel in the shadow of the limiter.

Instead of using current carrying RF conductors positioned between the plasma boundary and the vacuum vessel wall, the conducting surface around a slot cut in the vessel wall is used for the slot type antenna. This removes the 'image' RF current at the vessel surface that lowers the efficiency of loop type ICRF antennas. On the other hand, the antenna elements, being the source of additional impurities, are removed from the near-plasma region. The design of the slot type antenna decreases its inductance (<0.1 μH) and, consequently, its input impedance. A slot type antenna of similar design was also applied in the TARA open trap for plasma production in the ICRF [28]. The properties of slot type antennas make them promising candidates for reactor scale fusion devices.

A number of experiments on RF plasma production using frame type antennas has been performed on the OMEGA toroidal device [26]. If about 200 kW of RF power is coupled to the plasma at f = 3.6 MHz, neutral gas (hydrogen) ionization is accomplished in t = 0.02–0.04 ms. During this time, a plasma with a density $\bar{n}_e = (0.5\text{–}1.0) \times 10^{13}$ cm^{-3} is built up; this plasma is uniform along the torus and has a bell type profile over the cross-section.

RF plasma production in the torus proved to be sufficiently efficient in a broad range of confining magnetic fields, $B_0 \approx 1\text{–}10$ kG, at initial hydrogen pressures $p_{H_2} = (0.1\text{–}2.0) \times 10^{-4}$ torr.

With RF power coupling to the OMEGA device, using an antenna having an asymmetric spectrum over the longitudinal wave numbers, $P_{rf}(k_\parallel)$, it was possible to produce a dense RF plasma, $\bar{n}_e \approx (1\text{–}8) \times 10^{12}$ cm^{-3}, with simultaneous ramp-up of the current in the plasma torus ($dI_p/dt \approx 3.0$ MA/s) when ion Bernstein (IB) waves ($\omega > \omega_{ci}$) and Alfvén waves ($\omega < \omega_{ci}$) travelling along the torus were excited [29]. With such a technique in this small toroidal device without rotational transform, a quasi-steady tokamak regime was achieved with a safety factor q = 4 at the plasma boundary owing to ICRF current drive.

2.2. Experiments on the CHS torsatron

In the $\ell = 2$ CHS torsatron (R = 100 cm, $\bar{a}$ = 20 cm), a number of experiments on plasma production in EC [16] and IC [32] ranges of frequencies have been performed. In contrast to the hollow profile of the plasma produced with the microwave technique ($n_e(0)/n_{e\,max} \sim 40\%$), a plasma with a flattened profile was obtained with ICRH [32]. According to Ref. [39], in these experiments a Nagoya type-III antenna was used that was equivalent to the Khar'kov frame type antennas employed in earlier experiments (1971–1976, see Refs [40, 19]). In contrast to these antennas, the Nagoya type-III antenna has an electrostatic screen that is used to diminish the poloidal component of the alternating electric field. The possibility to efficiently produce a plasma with a density $\bar{n}_e \approx 6 \times 10^{12}$ cm^{-3} in a broad range of confining magnetic fields ($\Omega = \omega/\omega_{ci} \approx 0.33\text{–}1.0$) in the regime of slow wave excitation was demonstrated in CHS [32]. According to Ref. [32], the slow wave absorption was due to Landau damping.

2.3. Plasma production mechanisms

To clarify the physical mechanisms forming the basis of plasma production by the ICRF technique, the conditions of neutral gas RF breakdown, ionization and density accumulation of the plasma produced have been studied in the OMEGA toroidal device and in the URAGAN-2 and URAGAN-3 stellarators [24, 25, 31, 41].

It was found that to achieve neutral gas breakdown it is necessary to have a longitudinal (along the magnetic

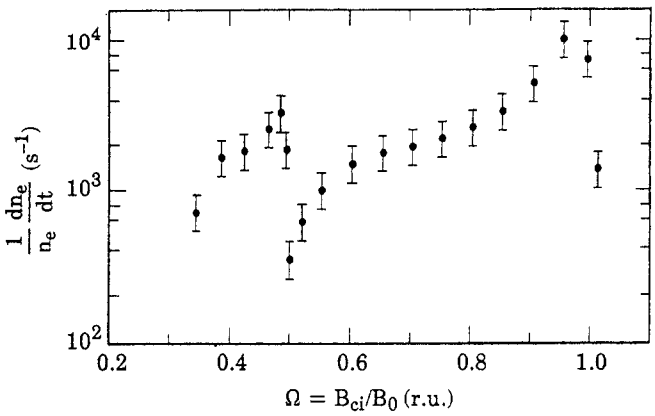

FIG. 1. Hydrogen ionization rate at the RF breakdown stage versus the confining magnetic field (URAGAN-2 stellerator, f = 10 MHz, $P_{rf} \approx$ 200 kW, $p_{H_2} = 6 \times 10^{-5}$ torr).

field lines) electrical component ($\tilde{E}_\parallel = (\vec{\tilde{E}} \cdot \vec{B}_0)/B_0$) in the structure of the RF field radiated by antennas which causes stronger electron oscillations than other RF field components. It was found experimentally that RF breakdown and gas preionization took place only for certain values of the antenna RF current, $I_{min} < \tilde{I}_{rf} < I_{max}$ [41]. Gas breakdown could not occur when $\tilde{I}_{rf} < I_{min}$ and $\tilde{I}_{rf} > I_{max}$. The low current limit can be understood in terms of the electron oscillation energy required to ionize the gas. The high current limit was explained using analytic estimates for the destruction of the RF potential formed by the antenna near-field (more details are given in Section 3.2).

The growth rate of the plasma density at RF breakdown, experimentally measured in the URAGAN-2 racetrack stellarator, has a resonant behaviour at the confining value of the magnetic field B_0 (Fig. 1). Two resonances manifest themselves: the first one is at $\Omega = 0.5$ and the second at $\Omega = 1$. The first resonance has a three times smaller amplitude of $(1/n_e)/(\partial n_e/\partial t)$ than the second one. This can be explained by cyclotron acceleration of heavy minority ions [20] — molecular H_2^+ or deuterium and helium ions — which may also appear in the discharge. Non-linear cyclotron acceleration of hydrogen ions at half-integer cyclotron harmonic frequencies is also possible [29].

The highest rate of plasma production ($(1/n_e)(\partial n_e/\partial t) \approx 10^4\ s^{-1}$) is achieved at the $\Omega = 1$ resonance. Besides the electron impact ionization mechanism, ion impact ionization is also possible. For the latter to be effective, it is necessary to have relatively high energy ions (5–100 keV); such ions can be produced in the IC region. Note that such high energy ions were registered at discharge startup in an ICRF experiment [22]. The mechanism of the interaction of ions with the RF field depends strongly on whether or not the value of the magnetic field varies along the magnetic field line. In conventional stellarators, this value changes along magnetic field lines forming local mirrors. In such devices, IC heating proceeds as a diffusion in the ion velocity space. In machines with a magnetic field changing weakly along the magnetic field lines (tokamaks before Ohmic discharge startup and straight parts of racetrack stellarators), there may be a stronger interaction mechanism of ions with the RF field, namely direct ion acceleration at the IC resonance surface.

There are three different cases of this mechanism (see Ref. [42]):

(a) A strong RF field (low neutral gas density), with an amplitude $v_{i+}^* = e\tilde{E}_+/m_i\nu_c > 3 \times 10^8$ cm/s ($\tilde{E}_+ = \tilde{E}_x + i\tilde{E}_y$, $\nu_c = n_a\langle\sigma_c v\rangle$ — charge exchange collision frequency): In this case, near a cyclotron resonance surface, ions are accelerated to high energies (>100 keV). The ionization rate due to these ions is small. Because of collisional scattering and a decrease of the slowing down rate with increasing ion energy, the energy of these ions is determined by non-linear effects or ion losses due to magnetic drift. Near the cyclotron resonance surface, ions are not accelerated but oscillate with an amplitude $\tilde{v}_{i+} = e\tilde{E}_+/m_i\,|\omega - \omega_{ci}|$. Since $\tilde{v}_{i+} < v_{i+}^*$, there exists a region where $\tilde{v}_{i+} \sim 10^8$ cm/s; in this region, effective ionization by ion impact occurs.

(b) A low RF field (high neutral gas density), with $v_{i+}^* < 5 \times 10^7$ cm/s: In this case, the ion energy level is not sufficient for impact ionization.

(c) An intermediate RF field, with $v_{i+}^* \sim 10^8$ cm/s: In this case, the ionization rate is high and reaches a peak value at the IC resonance surface. The width of the high ionization rate region is determined by the condition $|\omega - \omega_{ci}| \sim \nu_c$.

Probe measurements of RF fields in a buildup plasma showed that the plasma production process was accompanied by intensive excitation of RF oscillations in the plasma torus volume; these oscillations were first of the electrostatic type and then of the electromagnetic type [31]. A theoretical analysis of the dispersion properties of the oscillations registered [20–22, 24–26] showed that, beginning with a certain minimal value of the plasma density determined by the condition $\omega = \omega_{pe}$, short wavelength or slow Alfvén waves were excited first, and then, with increasing density, electromagnetic waves, or fast Alfvén waves and FMS waves were excited (the Alfvén wave at $\omega \leq \omega_{ci}$ is also called the IC wave).

In experiments performed in stellarator type devices [20–22, 31, 32] it was found that the range of values of the confining magnetic field at which dense plasma production was possible was determined by the efficiency of wave excitation, i.e. it was conditioned by the spectral properties of the antennas. Antennas with a narrow $k_\parallel$ spectrum of radiated RF power, $P_{rf}(k_\parallel)$, produced a dense ($\bar{n}_e > 10^{13}$ cm^{-3}) plasma in a narrower range of changes of the confining magnetic field compared with antennas having a broad $k_\parallel$ spectrum. Production of dense plasma in toroidal magnetic devices by the ICRF technique ($\omega < \omega_{ci}$) was achieved only in regimes of efficient excitation of Alfvén waves (IC waves) and only when they approached the local Alfvén resonance (AR) region. In the AR region the electric and magnetic RF field amplitudes increased sharply and the plasma loading resistance also increased, indicating enhancement of wave absorption in the plasma [26]. Theoretical analysis showed that in these experiments in the AR region, conversion of fast waves to slow waves took place, and the strong absorption of the latter by electrons heated them and led to fuller ionization of the neutral gas in the total volume of the plasma torus.

On increasing the level of the coupled RF power, non-linear mechanisms of Alfvén wave and IC wave energy absorption became possible [24, 26, 43, 44] together with linear ones.

The studies performed have helped establish the general features of plasma ICRF production in toroidal magnetic devices and to discriminate two stages in the plasma production process on increasing the plasma density (from the viewpoint of RF power coupling):

— *Non-wave stage* (RF breakdown): neutral gas ionization by electrons in the longitudinal electric field of the antenna (in the IC region, the ions may also contribute to the ionization together with electrons), and spreading of the low density plasma along the magnetic field lines of the device.
— *Wave stage:* ionization of the total gas volume over the whole torus, due to strong absorption by electrons of slow waves excited either directly by the antenna or as a result of fast wave conversion in the AR region.

Successive excitation of slow and fast Alfvén waves with increasing density is accomplished in the 'relay race' mode regime because of the broad $k_\parallel$ spectrum of the RF power radiated by antennas. In subsequent experiments, the optimum conditions for RF discharge formation regarding the neutral gas pressure and the shape and amplitude of the RF pulse [30, 31] were determined.

In URAGAN-2, the application of the developed ICRF plasma production technique made it possible to obtain a plasma with a density $\bar{n}_e = 7 \times 10^{13}$ cm^{-3} with gas puffing [24]. With the same technique, a two-ion plasma with a controlled ratio of the ion component concentrations was obtained [20, 24, 43].

3. INITIAL PLASMA PRODUCTION IN LARGE SCALE TOKAMAKS BY THE ICRF TECHNIQUE

3.1. Confining magnetic configuration

As is known, it is not possible to confine a plasma with a pure toroidal magnetic field without a poloidal field. The vertical electric field due to charge separation by the gradient and centrifugal drifts in the toroidal magnetic field causes fast plasma movement to the walls of the vacuum vessel. The vertical magnetic field improves the confinement. Its minimum value is determined by the plasma pressure (see Refs [45–47]):

$$B_\perp \geq \sqrt{8\pi n_e k (T_e + T_i)\, a/R} \qquad (1)$$

where a is the plasma radius and R is the major radius of the torus. Two channels of particle and energy losses exist — losses due to the electric drift and losses due to the plasma motion to the wall along the magnetic field lines. The lifetime of particles due to the first process is

$$\tau_\perp \approx \frac{aR}{v_{Te}^2} \frac{\omega_{ce}^2}{(\nu_{en} + \nu_{ei})} \left(\frac{B_\perp}{B_0}\right)^2 \qquad (2)$$

If the value of $B_\perp$ is chosen according to Eq. (1), for a plasma with $n_e \approx 10^{12}$–10^{13} cm^{-3} and $T_e \approx 100$ eV, then at all production and heating stages the second process (losses along the magnetic field lines) would be dominant. The lifetime of particles determined by plasma losses along the magnetic field lines is

$$\tau_\parallel = \frac{a^2 \nu_{in}}{c_s^2} \left(\frac{B_0}{B_\perp}\right)^2 \quad \text{for} \quad \frac{a\nu_{in}}{c_s} \frac{B_0}{B_\perp} \gg 1 \qquad (3.1)$$

$$\tau_\parallel = \frac{a}{c_s} \frac{B_0}{B_\perp} \quad \text{for} \quad \frac{a\nu_{in}}{c_s} \frac{B_0}{B_\perp} \ll 1 \qquad (3.2)$$

(c_s is the ion sound velocity) depending on the relation between the ion mean free path in the neutral gas, $\lambda = c_s/\nu_{in}$, and the length of the field line, $L_0 = a(B_0/B_\perp)$. In the case of $\lambda \ll L_0$, the ions drift, and their transport rate is determined by collisions with

neutrals. If $\lambda \gg L_0$, then the ions move along the magnetic field lines to the vessel wall under the action of the ambipolar potential, without collisions.

3.2. Neutral gas RF breakdown

Gas breakdown is accomplished by electrons gaining the energy necessary for ionization in the longitudinal electric RF field $\tilde{E}_\parallel$. In the absence of plasma, the RF field is localized near the antenna, and its longitudinal electrical component is not shielded by charged particles ($\tilde{E}_\parallel \sim \tilde{E}$). Under the action of the RF field, the electrons moving along the magnetic field lines oscillate with frequency ω and with velocity $\tilde{v}_{e\parallel} = e\tilde{E}_\parallel/m_e\omega$. The electrons perform slow motions under the action of the RF potential [41], $\Phi_{rf} = e^2\tilde{E}_\parallel^2/4m_e\omega^2$. Since at RF breakdown the waves do not propagate in the torus ($\omega_{pe} < \omega$), the RF potential does not vanish only near the antenna system. The distribution of the RF potential along the torus is schematically shown in Fig. 2 for two types of frame antenna. In case (a), one extended potential well is formed along the torus circumference. In case (b), another potential well of smaller size arises near the antenna. Breakdown can occur only owing to electrons that are born inside the antenna near-field region. The energy of these electrons is of the order of the oscillation energy in the RF field. The gas preionization process can proceed if the oscillation energy exceeds the ionization energy threshold

$$\frac{m_e \tilde{v}_{e\parallel}^2}{2} \approx \epsilon_H \qquad (4)$$

where $\epsilon_H = 15.2$ eV for the hydrogen molecule. In case (a), low energy electrons born at the bottom of the extended potential well remain trapped there. These electrons cannot penetrate into the antenna near-field region and cannot acquire the energy needed for gas ionization. The ionization efficiency will be lower by a factor of $2\pi R/L_\parallel$ compared with the case of a uniform RF field distribution along the torus ($L_\parallel$ is the dimension of the antenna near-field region).

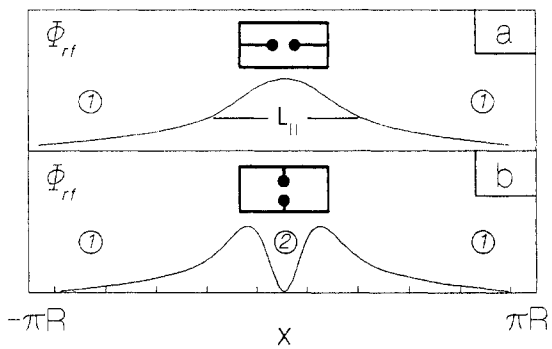

FIG. 2. RF potential distribution along the magnetic field line for two types of frame antennas.

In case (b), the breakdown proceeds in another way. In this case, another potential well is formed. Unlike the first well, the additional well is small and is located in the antenna near-field region. Electrons trapped in this well continuously oscillate and, when condition (4) is met, effectively ionize the neutral gas. The electrons due to ionization events also become trapped in this well. Thus, the breakdown process in this case proceeds like that in the case of uniform RF field distribution.

It has to be noted that if the oscillation amplitude of electrons in the RF field, $\tilde{x} = \tilde{v}_{e\parallel}/\omega$, becomes comparable to the size of the RF field localization region $L_\parallel$, the RF potential is destroyed.

From the condition of a maximum ionization rate and of the existence of an additional RF potential well, it is possible to write the RF breakdown criterion in the following form [41, 48]:

$$\omega\sqrt{2m_e\epsilon_H}/e < \tilde{E}_\parallel < \omega^2 m_e L_\parallel/2e \qquad (5)$$

With $\omega = 1.88 \times 10^7$ s^{-1} and $L_\parallel = 2$ m, we obtain 2 V/cm $< \tilde{E}_\parallel <$ 20 V/cm.

3.3. Wave stages of an RF discharge

On increasing the plasma density ($\omega_{pe} > \omega$), the condition of slow wave (being the short wavelength part of the Alfvén branch of oscillation) propagation arises, the dispersion law for which is determined by the expression

$$N_\perp^2 = -\frac{\epsilon_{33}}{\epsilon_{11}}(N_\parallel^2 - \epsilon_{11}) \qquad (6)$$

where ϵ_{11} and ϵ_{33} are the components of the cold plasma dielectric tensor. At $\omega_{pe}^2 > \omega^2$, the slow wave polarization is such that $\tilde{E}_\parallel/\tilde{E}_\perp \ll 1$. For this reason, a lower ionization rate with respect to the breakdown stage should be expected.

On increasing the plasma density, the perpendicular wavelength of the slow wave becomes much less than the plasma radius, and the WKB approximation becomes correct. This approximation gives $\tilde{E}_\parallel \propto n_e^{-1/2}$, i.e. the value of the $\tilde{E}_\parallel$ amplitude is higher at the points of the density profile where the value of the density is lower. Note that the higher the value of the $\tilde{E}_\parallel$ amplitude, the higher is the ionization rate. Thus, with increasing density, a self-consistent density profile is formed in which the $\tilde{E}_\parallel$ amplitude distribution is uniform [49].

This self-consistent density profile occupies the bulk of the confinement volume and its shape depends on the structure of the antenna RF current.

For $n_e \ll n_H$ (n_H is the hydrogen molecular neutral gas density), the processes of resonant charge exchange of molecular ions and of H_3^+ ion formation determine the transport. For $n_H = 10^{12}$ cm^{-3} from Eq. (3.1), a lifetime estimate can be obtained by using $\nu_{in} \approx 10^{-9}\, n_H\ s^{-1}$, where n_H is in cm^{-3} ($\langle \sigma v \rangle \approx 10^{-9}$ cm^3/s). This estimate gives $\tau_\parallel \approx 10$ s, i.e. the loss of low density plasma is negligibly small.

We now discuss briefly the ionization mechanism. When condition (4) is fulfilled, the major part of the electrons have energies exceeding the ionization threshold. If the RF field strength is below the value defined by Eq. (4), the electrons may gain sufficient energy for ionization because of elastic collisions with hydrogen molecules. In this case, ionization is accomplished at low electron temperature, $kT_e < \epsilon_H$, owing to electrons from the distribution function tail. In spite of the decreased ionization rate compared with that in the non-wave (breakdown) stage, the density of the produced plasma grows continuously owing to small losses of charged particles.

When the plasma density is further increased, the conditions for excitation of global resonances are fulfilled, first for Alfvén waves and, at higher density, also for FMS waves. The $\tilde{E}_\parallel$ component of the RF field in these waves is very small and there is a rather weak direct interaction with electrons; however, another possible mechanism has been realized in a number of experiments [20, 21, 24–26], namely conversion of Alfvén waves to slow waves in the AR layer.

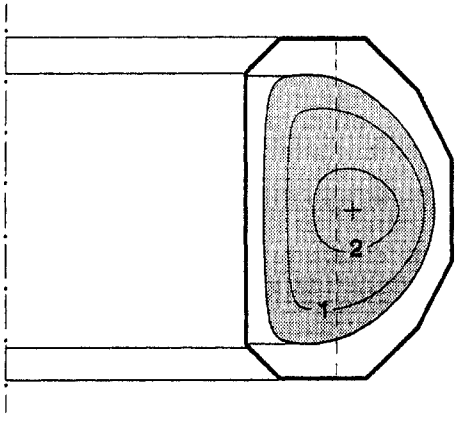

FIG. 3. Location of AR surfaces in a target plasma column (solid lines) for two values of the toroidal mode number ($n_2 > n_1$). The dashed line indicates a magnetic surface in a tokamak before the startup of the Ohmic discharge ($B_\perp \neq 0$).

In the toroidal magnetic field, the Alfvén resonance condition is as follows [50–52]:

$$\epsilon_{11} = N_\parallel^2 = \left(\frac{n}{R}\,\frac{c}{\omega}\right)^2 \tag{7}$$

where n is the toroidal mode number. The AR surfaces defined by condition (7) in the meridian cross-section are closed curves on which ϵ_{11} is constant (Fig. 3). When a vertical magnetic field $B_\perp$ is superimposed on the toroidal field B_0, the magnetic field lines are not closed. They intersect the plasma column as well as the vessel wall. According to Ref. [51], the AR surfaces in such a case are surfaces of revolution which themselves include magnetic field lines; they differ slightly from cylinders with r = const (Fig. 3). We use Eq. (4) from Ref. [50] to obtain the AR condition in a tokamak with a vertical magnetic field before start of the Ohmic discharge:

$$\frac{d}{dz}\,\frac{1}{\epsilon_{11}}\,\frac{d}{dz}\,y + \frac{\omega^2}{c^2}\,\frac{B_0^2}{B_\perp^2}\,y = 0 \tag{8}$$

where y is determined by the formula for the toroidal magnetic strength component of the RF field:

$$H_\phi = \frac{y}{(r - r_{AR})} \exp\left(-in \int \frac{B_0}{B_\perp}\,\frac{dz}{r} + in\phi\right) \tag{9}$$

Here we use cylindrical co-ordinates: $r \equiv R$ is the major radius, ϕ is the toroidal angle and z is the co-ordinate along the major toroidal axes. The identity $r = r_{AR}$ determines the AR surface. Together with boundary conditions, Eq. (8) forms the eigenvalue problem. The eigenfunctions of this problem can be used to evaluate the RF field asymptotics in the vicinity of the AR surface using relation (9). When the condition $(\omega^2/c^2)/(B_0^2/B_\perp^2)\,\epsilon_{11} \gg 1$ is met, the WKB approximation can be used for solving Eq. (8). In this case,

$$H_\phi = \frac{C\sqrt[4]{\epsilon_{11}}}{(r - r_{AR})} \left\{\exp\left[i\,\frac{B_0}{B_\perp}\int dz\left(\frac{\omega}{c}\sqrt{\epsilon_{11}} - \frac{n}{r}\right)\right] + \exp\left[-i\,\frac{B_0}{B_\perp}\int dz\left(\frac{\omega}{c}\sqrt{\epsilon_{11}} + \frac{n}{r}\right) + i\Phi_1\right]\right\} \times \exp(in\phi) \tag{10}$$

The eigenvalue spectrum is determined from the quantization condition

$$\frac{\omega}{c}\,\frac{B_0}{B_\perp}\int \sqrt{\epsilon_{11}}\,dz = \pi j + \Phi_2 \tag{11}$$

where j is an integer and Φ_1 and Φ_2 are the constants of order π, which depend on the boundary conditions. We do not define these constants explicitly. Formula (11) determines the AR condition; from this formula, one can evaluate the r_{AR} values.

The RF field (Eq. (10)) oscillates, with z fast except in the vicinity of stationary phase points. The locations of these points are determined by a condition that coincides with condition (7), which must be taken at the point $r = r_{AR}$. Note that the stationary phase condition does not depend on the j values.

The resonance structure described by Eqs (10) and (11) is sustained when the separate resonances are far from one another and do not overlap. Resonances can overlap because of their finite width, which is due to energy absorption or mode conversion. An estimate of the broadening of the resonance due to the conversion mechanism is

$$\Delta_c = \left(\frac{\partial k_\perp^2}{\partial r}\right)^{-1/3} \tag{12}$$

The spacing between adjacent resonances is estimated using Eq. (11):

$$\Delta = \frac{B_\perp}{B_0} \frac{\sqrt{1-\Omega^2}}{\Omega} \frac{c}{\omega_{pi}} \tag{13}$$

Taking into account effects of the finite electron mass, the condition for resonances to overlap owing to conversion is

$$\frac{\Delta}{\Delta_c} = \frac{B_\perp}{B_0} \left(\frac{1-\Omega^2}{\Omega^2} \frac{m_i}{m_e} \frac{R}{a} \frac{1}{n}\right)^{1/3} \ll 1 \tag{14}$$

It is evident that in the case under investigation, condition (14) is fulfilled because $B_\perp/B_0$ is very small. Therefore, $B_\perp$ can be neglected and condition (7) can be used to find the location of the AR surface in a tokamak plasma in the startup phase of a discharge. Condition (7) for a fixed $k_\parallel$ value can be fulfilled when the plasma density exceeds some critical value, because $\epsilon_{11} \sim n_e$. For higher density values, the location of the AR surface in the plasma column is changed. This shift of the AR surface depends on the plasma density profile. It is not quite clear how the radial profile of the plasma density changes when it is produced by the ICRF technique. If the plasma is assumed to have a bell shaped profile, as observed in small scale devices [26], then an AR surface emerges near the plasma centre when the density reaches the critical value. When the density is further increased, the AR surface expands and moves to the plasma periphery. At the same time, for a higher $k_\parallel$ value ($k_{\parallel 2} > k_{\parallel 1}$, Fig. 3) an AR surface emerges in the plasma centre. The newly formed resonances behave similarly. Consequently, antennas forming a broad $k_\parallel$ spectrum of the radiated RF power may provide the dynamic process for a 'relay race' of resonances and for plasma density growth.

The wave stage of plasma production can be achieved with an efficient mechanism of excited wave energy absorption. The slow wave propagating along the radius and along the torus is absorbed by electrons and heats them. The absorption mechanism consists of Coulomb collisions of electrons with heavy particles. The Alfvén waves and the FMS waves are absorbed only by charge exchange collisions, which absorption is still very weak. The damping length over the radius of the slow wave is

$$L = \frac{1}{\mathrm{Im} k_\perp} \approx \sqrt{m_e/m_i} \frac{\omega}{\omega_{ci} k_\parallel \nu_{ei}} \tag{15}$$

with $\omega < \omega_{ci}$ and $k_\parallel c/\omega > \omega_{pi}/\omega_{ci}$. The estimates show that, at $n_e \approx 10^{12}$ cm^{-3} and $T_e \approx 5$–100 eV, the absorption of slow waves is strong, $L \ll a$, even for long waves with $k_\parallel = 10^{-3}$–10^{-2} cm^{-1} (for such waves, Landau damping is negligibly small). Therefore, energy can be transported into the plasma core only by Alfvén resonances.

3.4. Neutral gas burnout and heating of fully ionized plasma

The neutral gas burnout stage ($n_e \sim n_a$) is the most important stage because it is characterized by considerable energy losses connected with the excitation and ionization of neutral atoms. In the heating stage of a fully ionized plasma, the energy losses connected with transport become dominant. We have analysed the processes occurring at these stages of plasma production with a numerical method in the framework of the 0-D model. The model includes the energy balance of electrons, ions and atoms as well as particle balance. The energy balance equations are as follows:

$$\frac{3}{2}\frac{d(n_e T_e)}{dt} = P_{rf} - \frac{3}{4}\epsilon_i \langle\sigma v\rangle_e n_e n_a - \epsilon_i \langle\sigma v\rangle_i n_e n_a - \frac{k_c (T_e - T_i) n_e^2}{T_e^{3/2}} - \frac{(T_e + eU_{amb}) n_e}{\tau_\parallel} \tag{16}$$

$$\frac{3}{2}\frac{d(n_e T_i)}{dt} = \frac{k_c (T_e - T_i) n_e^2}{T_e^{3/2}} - (T_i - T_a)\langle\sigma v\rangle_c n_e n_a - \frac{3}{2}\frac{n_e T_i}{\tau_\parallel} \tag{17}$$

$$\frac{3}{2}\frac{d(n_a T_a)}{dt} = (T_i - T_a)\langle\sigma v\rangle_c n_e n_a - 3\frac{n_a T_a}{a}\sqrt{T_a/m_a} \tag{18}$$

where $\langle\sigma v\rangle_e$, $\langle\sigma v\rangle_i$ and $\langle\sigma v\rangle_c$ are the rate coefficients of excitation, ionization and charge exchange, respec-

tively, P_{rf} is the power density of electron RF heating, $k_c = 2.44 \times 10^{-8}$ cm^3·eV$^{1/2}$·s^{-1}, $\epsilon_i = 13.6$ eV, $U_{amb} = 3.5\ T_e/e$ and $\tau_\parallel$ is determined by expressions (3.1) and (3.2). The electron energy balance (16) includes the RF heating, energy losses due to radiation and ionization, Coulomb energy exchange with ions and confinement losses. The ion energy balance (17) includes the energy exchange with electrons and atoms due to charge exchange as well as confinement losses. The atom energy balance (18) includes the energy exchange with ions and the convective transport of energy to the wall of the vacuum chamber. Particle balance equations have the form

$$\frac{dn_e}{dt} = \langle\sigma v\rangle_i n_e n_a - \frac{n_e}{\tau_\parallel} \qquad (19)$$

$$n_e + n_a = \text{const} \qquad (n_e = Zn_i,\ Z = 1) \qquad (20)$$

The dynamics of the system with a constant number of particles has been considered (Eq. (20)), i.e. the 'hot' ion lost at the wall has been replaced in the confinement volume by the 'cold' atom (assumption of complete recycling).

The calculations have been performed for a reactor scale tokamak with a = 2 m, R = 5 m, $B_0 = 5$ T, $B_\perp = 100$ G. Figures 4–7 show the results of calculations describing the temporal evolution of the parameters of the plasma produced at the stages of neutral gas burnout and of heating of fully ionized plasma for different values of coupled RF power and gas fill pressure. Analysis of the given dependences shows that neutral gas burnout ($n_e \sim n_a$) is accomplished at $T_e \approx 3$–5 eV, which is considerably lower than the ionization threshold. The main loss channel of electron

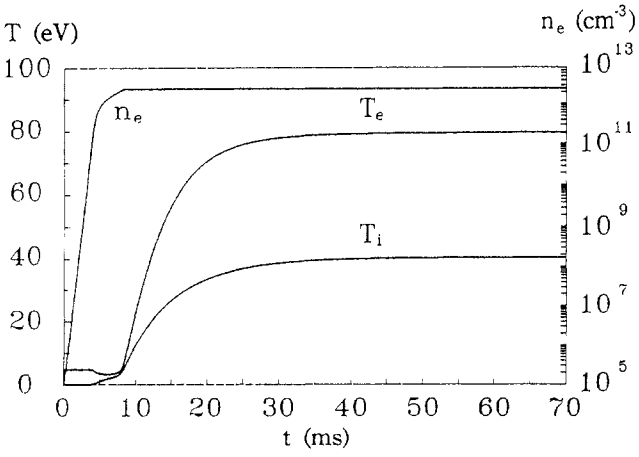

FIG. 4. Temporal evolution of the target plasma parameters in a reactor scale tokamak for $P_{rf} = 6$ MW and $n_a = 3 \times 10^{12}$ cm^{-3}.

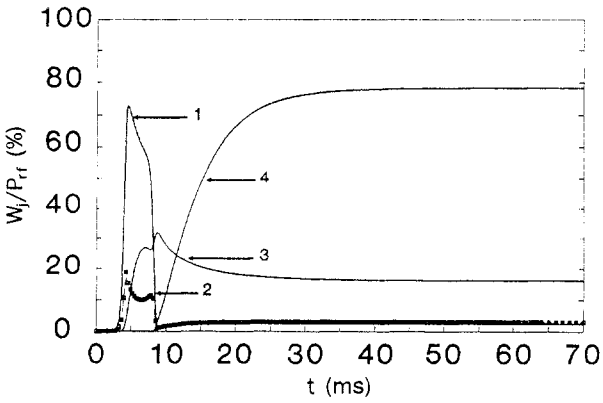

FIG. 5. Temporal evolution of the ratio of electron energy loss power, W_j, to RF heating power, P_{rf}: $j = 1$ — radiation losses; $j = 2$ — ionization losses; $j = 3$ — Coulomb energy exchange with ions; $j = 4$ — transport losses ($P_{rf} = 6$ MW, $n_a = 3 \times 10^{12}$ cm^{-3}).

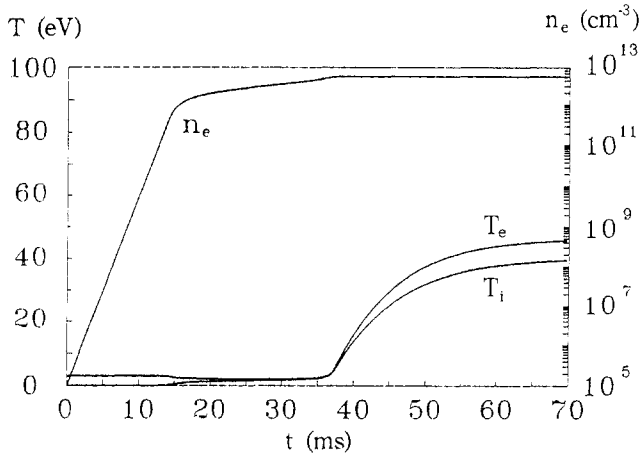

FIG. 6. Same as Fig. 4 for $P_{rf} = 6$ MW and $n_a = 6 \times 10^{12}$ cm^{-3}.

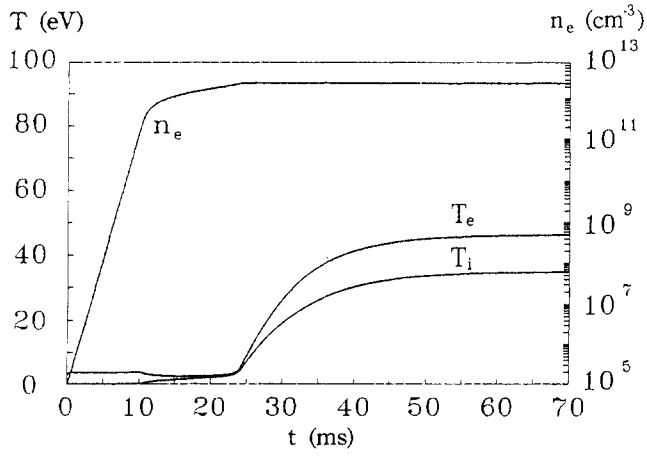

FIG. 7. Same as Fig. 4 for $P_{rf} = 3$ MW and $n_a = 3 \times 10^{12}$ cm^{-3}.

energy at this stage is connected with radiation; it contains about 70% of the input RF power (curve 1, Fig. 5). Coulomb energy exchange with ions involves about 20% of the input power (curve 3) and ionization 10%. Losses associated with confinement are negligible (curve 4). Note the strong increase of the duration of burnout with the increase of the initial neutral gas pressure (Fig. 6) and the decrease of the coupled RF power (Fig. 7).

According to the results of calculations, to produce a plasma with a density $n_e \approx 3 \times 10^{12}$ cm^{-3}, it is sufficient to couple about 3 MW of RF power to electrons; to produce a plasma with a density $n_e \approx 6 \times 10^{12}$ cm^{-3}, more than 6 MW of RF power is required.

The stage of heating of a fully ionized plasma is characterized by enhanced electron energy losses along the magnetic field lines (about 80% of the input RF power, curve 4, Fig. 5). Because of the moderate value of the plasma density ($n_e \sim 10^{12}$ cm^{-3}) the rate of energy exchange with ions is low (about 20%).

At this stage of an RF discharge the electron temperature grows continuously, up to the flat-top value. The time of electron temperature growth t_s is governed by the RF power level for a given value of the plasma density: $t_s \approx 5.7$ ms for $P_{rf} = 6$ MW and $t_s \approx 8.5$ ms for $P_{rf} = 3$ MW at $n_e = 3 \times 10^{12}$ cm^{-3}. According to Eqs (3.2) and (16), the flat-top value of the electron temperature depends on the ratio P_{rf}/n_e, $T_e \propto (P_{rf}/n_e)^{2/3}$; at $P_{rf} = 6$ MW and $n_e = 3 \times 10^{12}$ cm^{-3}, the electron temperature amounts to 80 eV.

Note that the model considered ignores the role of impurities. Their contribution to the energy balance is negligible at all stages of plasma buildup except for the plasma heating stage. However, the confinement properties of the magnetic configuration considered degrade strongly with increasing electron temperature. Therefore, taking into account the radiation energy losses due to impurities leads to less changes of the electron temperature evolution compared with those of a tokamak or stellarator having better confinement.

Thus, analysis of the numerical calculations shows that a fully ionized plasma with $n_e \approx 3 \times 10^{12}$ cm^{-3} and $T_e \approx 80$ eV can be produced in a reactor scale tokamak before startup of an Ohmic discharge with an input RF power of only 3–6 MW.

3.5. Antenna system for plasma ICRF production in a reactor scale tokamak

Studies of the RF power coupling process for plasma buildup show that the electromagnetic antenna systems must meet a number of requirements regarding the structure of the radiated RF field and the spectral and energy properties. The RF currents in the antenna system must have components for RF breakdown near the antenna as well as components for the subsequent excitation of the waves when the density is increased; first the slow waves are excited and then the fast waves in the whole plasma torus [24]. On the other hand, to obtain high plasma densities, the wave stage of RF power coupling must be achieved in the 'relay race' mode regime [24, 25], i.e. the antennas must have broad spectra of the radiated RF power $P_{rf}(k_\parallel)$ over longitudinal wave numbers $k_\parallel$. The antennas also must have low inductance and, consequently, minimal input impedance in order to avoid high values of the RF voltage on the antenna elements.

It is advisable to use slot type antennas [21, 22] to accomplish RF preionization in reactor scale tokamaks (Fig. 8). As noted above, for the slot type antennas, no elements are installed between the plasma and the vessel wall. The conducting surface of the vacuum vessel around the slot cut in the wall is used for carrying RF current. Such antennas have a low inductance. Antennas of the slot type can be used to form an RF field structure with the $\tilde{E}_\parallel$ component necessary for neutral gas breakdown, resulting from the longitudinal RF current component carried along the slot edge, $\tilde{I}_\parallel$. Different schemes of RF power induction with slot type antennas make it possible to produce an RF potential distribution similar to that shown as case (a) in Fig. 2 for the top slot and the bottom slot (see Fig. 8) or similar to case (b) of Fig. 2 for the central slot at RF discharge startup. Moreover, the $\tilde{I}_\parallel$ component of the antenna RF current excites effectively the slow wave in the low density plasma. Since slot type antennas have the poloidal RF current component $\tilde{I}_\theta$, they can be used to excite Alfvén waves and FMS waves, with a further increase in plasma

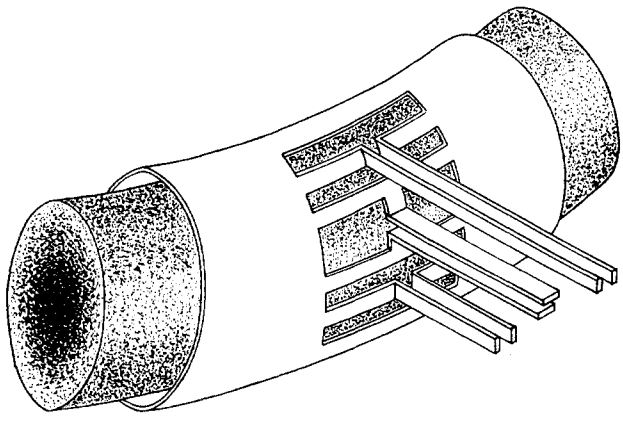

FIG. 8. Slot type antennas for a reactor scale tokamak.

density. Because of the absence of the radial RF current component $\tilde{I}_r$, the excitement of Alfvén waves and FMS waves is increased by a factor of $(1 + m^2/k_\parallel^2 a^2)^2$ in the proposed antennas (m being the poloidal mode number) compared with the usual loop type antennas [53]. Finally, the broad $k_\parallel$ spectrum of the RF power radiated by slot type antennas gives the possibility to accomplish the wave stages of plasma ICRF production in the 'relay race' mode regime.

The proposed antennas of the slot type can be used to realize all stages of RF discharges in the ICRF and to produce dense plasmas, and they are well adjusted to fusion reactor requirements.

The slot type antennas can be installed in one of the vacuum vessel ports, similar to antennas intended for auxiliary plasma heating systems, or slots can be cut directly in the first wall of the vacuum vessel without considerably diminishing the blanket volume behind the antenna (Fig. 8.)

4. CONCLUSIONS

In our studies we found that when plasma is produced with the RF technique in the ICRF the RF discharge passes a number of subsequent stages:

- Neutral gas RF breakdown stage ($n_e \ll n_a$) due to acceleration of electrons in the longitudinal (along the magnetic field lines) electric RF field of the antenna; in this stage ($\omega_{pe} < \omega$) the RF potential generated by the antenna plays an important role;
- Gas preionization stage ($n_e < n_a$), in which, on increasing the plasma density ($\omega_{pe} > \omega$), first slow waves are excited and then global resonances of the Alfvén wave, local Alfvén resonances and, at higher densities, global resonances of the FMS wave;
- Neutral gas burnout stage ($n_e \sim n_a$), in which all above mentioned waves are excited and which is characterized by the largest energy losses.

The mechanism of RF power absorption in the wave stages is strong collisional damping of slow waves on electrons, excited directly by the antenna or as a result of Alfvén wave conversion in the local AR regions.

In the wave stages of an RF discharge, as distinct from the RF breakdown stage, volume ionization over the whole torus is accomplished. High density plasma can be produced only in the 'relay race' mode regime of slow and fast wave excitation because of the broad $k_\parallel$ spectrum of the RF power radiated by the antenna.

The studies performed also show that this RF technique of plasma production is weakly sensitive to the properties of the confining magnetic configuration in all stages of an RF discharge, including neutral gas burnout. The only requirement regarding the confining magnetic configuration is that plasma equilibrium must be ensured. Because of this, the plasma production technique considered is universal. It can be applied in stellarators and open magnetic traps, as well as in tori without rotational transform (tokamaks before the start of the Ohmic discharge).

The results of the studies performed show that RF fields in the IC (Alfvén) frequency range can be used to produce target plasmas in reactor scale tokamaks. This plasma production technique has been suggested for the ITER tokamak.

Numerical simulation shows that in ITER a target plasma can be produced with a density $\bar{n}_e \approx 3 \times 10^{12}\,cm^{-3}$ for 3–6 MW input RF power at $f \approx 3$ MHz. This level of RF power is sufficient not only for full ionization of the neutral gas but also for heating the plasma to electron temperatures of ≈ 80 eV.

The coupling of RF power of such a level presents no engineering difficulties. An array of slot antennas can be used for this purpose.

The ICRF plasma production technique is promising for application to large scale devices. For its realization, a number of problems have to be solved, entailing

- studies on target plasma ICRF production in tokamaks of middle and large scales and a more complete experimental database on the evolution of all stages of RF plasma production;
- development of numerical codes accounting self-consistently for the mutual effect of antenna–plasma coupling and of the plasma production process at all stages of plasma density growth.

REFERENCES

[1] PISTUNOVICH, V.I., SHATALOV, G.E., in Itogi Nauki i Tekhniki, Ser. Fizika Plazmy, Vol. 2, VINITI, Moscow (1981) 166 (in Russian).

[2] KNOEPFEL, H., SPONG, D.A., Nucl. Fusion **19** (1979) 785.

[3] BESEDIN, N.T., KUZNETSOV, Yu.K., PANKRATOV, I.M., Fiz. Plazmy **12** (1986) 759 (in Russian); Sov. J. Plasma Phys. **12** (1986) 436.

[4] THOMAS, P.R., CHRISTIANSEN, J.P., EJIMA, S., in Controlled Fusion and Plasma Physics (Proc. 12th Eur. Conf. Budapest, 1985), Vol. 9F, Part I, European Physical Society (1985) 283.

[5] MOISEENKO, V.E., Ukr. Fizich. Zh. **35** (1990) 214 (in Russian).

[6] PENG, Y.-K.M., BOROWSKI, S.K., KAMMASH, T., Nucl. Fusion **18** (1978) 1489.
[7] MIRNOV, S.V., in Fizicheskie Protsessy v Plazme Tokamaka, Energatomizdat, Moscow (1985) 56 (in Russian).
[8] GILGENBACH, R.M., READ, M.E., HACKETT, K.E., et al., Nucl. Fusion **21** (1981) 319.
[9] HOLLY, D.J., PRAGER, S.C., SHEPARD, D.A., SPROTT, J.C., Nucl. Fusion **21** (1981) 1483.
[10] MOTOJIMA, O., SANO, F., SATO, M., et al., Nucl. Fusion **25** (1985) 1783.
[11] LLOYD, B., EDLINGTON, T., ALCOCK, M.W., et al., in Controlled Fusion and Plasma Heating (Proc. 13th Eur. Conf. Schliersee, 1986), Vol. 10C, Part II, European Physical Society (1986) 266.
[12] ALIKAEV, V.V., BORSHCHEGOVSKIJ, A.A., CHIST'AKOV, V.V., et al., in Plasma Physics and Controlled Nuclear Fusion Research 1986 (Proc. 11th Int. Conf. Kyoto, 1986), Vol. 1, IAEA, Vienna (1987) 533.
[13] D'YACHENKO, V.V., LARIONOV, M.M., LASHKUL, S.I., LEVIN, L.S., in Problems in Atomic Science and Techniques, Series Thermonuclear Fusion, No. 4, I.V. Kurchatov Inst. Atomic Energy, Moscow (1989) 20 (in Russian).
[14] ANISIMOV, A.I., VINOGRADOV, N.I., POLOSKIN, B.P., Zh. Tekh. Fiz. **45** (1975) 994 (in Russian).
[15] MOTOJIMA, O., MUTOH, T., SATO, M., et al., in Plasma Physics and Controlled Nuclear Fusion Research 1988 (Proc. 12th Int. Conf. Nice, 1988), Vol. 1, IAEA, Vienna (1989) 551.
[16] IGUCHI, H., and CHS Group, in Stellarator Physics (Proc. 7th Int. Workshop Oak Ridge, TN, 1989), IAEA-TECDOC-558, IAEA, Vienna (1990) 203.
[17] SÖLDNER, F., BROUQUET, P., DURVAUX, M., et al., in Controlled Fusion and Plasma Physics (Proc. 9th Eur. Conf. Oxford, 1979), UKAEA, Culham Laboratory, Abingdon, Oxfordshire (1979) 5.
[18] CHU, T.K., BELL, R., BERNABEI, S., et al., in Heating in Toroidal Plasmas (Proc. 4th Int. Symp. Rome, 1984), Vol. 1, Monotypia Franchi, Perugia (1984) 571.
[19] DIKIJ, A.G., KALINICHENKO, S.S., KALMYKOV, A.A., et al., Plasma Phys. **18** (1976) 577.
[20] DIKIJ, A.G., KALINICHENKO, S.S., KUZNETSOV, Yu.K., et al., in Plasma Physics and Controlled Nuclear Fusion Research 1976 (Proc. 6th Int. Conf. Berchtesgaden, 1976), Vol. 2, IAEA, Vienna (1977) 129.
[21] KALINICHENKO, S.S., KURILKO, P.I., LYSOJVAN, A.I., et al., in Controlled Fusion and Plasma Physics (Proc. 9th Eur. Conf. Oxford, 1979), UKAEA, Culham Laboratory, Abingdon, Oxfordshire (1979) 19.
[22] SHVETS, O.M., KALINICHENKO, S.S., LYSOJVAN, A.I., et al., Fiz. Plazmy **7** (1981) 485 (in Russian); Sov. J. Plasma Phys. **7** (1981) 267.
[23] DEMIRKHANOV, R.A., KIROV, A.G., ASTAPENKO, G.I., et al., in Plasma Physics and Controlled Nuclear Fusion Research 1982 (Proc. 9th Int. Conf. Baltimore, MD, 1982), Vol. 2, IAEA, Vienna (1983) 91.
[24] DIKIJ, A.G., KALINICHENKO, S.S., LYSOJVAN, A.I., et al., ibid., p. 581.
[25] SHVETS, O.M., DIKIJ, A.G., DIKIJ, I.A., et al., in Heating in Toroidal Plasmas (Proc. 4th Int. Symp. Rome, 1984), Vol. 1, Monotypia Franchi, Perugia (1984) 513.
[26] SHVETS, O.M., DIKIJ, I.A., KALINICHENKO, S.S., et al., Nucl. Fusion **26** (1986) 23.
[27] NAZAROV, N.I., PLYUSNIN, V.V., RANYUK, T.Yu., et al., Fiz. Plazmy **13** (1987) 1511 (in Russian); Sov. J. Plasma Phys. **13** (1987) 871.
[28] GOLOVATO, S.N., BRAU, K., CASEY, J., et al., Phys. Fluids **31** (1988) 3744.
[29] DIKIJ, I.A., KALINICHENKO, S.S., KITSENKO, A.B., et al., in Controlled Fusion and Plasma Heating (Proc. 15th Eur. Conf. Dubrovnik, 1988), Vol. 12B, Part II, European Physical Society (1988) 734.
[30] NAZAROV, N.I., PLYUSNIN, V.V., RANYUK, T.Yu., et al., Fiz. Plazmy **15** (1989) 1027 (in Russian); Sov. J. Plasma Phys. **15** (1989) 595.
[31] ZALESKIJ, Yu.G., KURILKO, P.I., NAZAROV, N.I., et al., Fiz. Plazmy **15** (1989) 1424 (in Russian); Sov. J. Plasma Phys. **15** (1989) 827.
[32] NISHIMURA, K., SHOJI, T., and CHS Group, in Stellarator Physics (Proc. 7th Int. Workshop Oak Ridge, TN, 1989), IAEA-TECDOC-558, IAEA, Vienna (1990) 265.
[33] KAYE, A., JACQUINOT, J., LALLIA, P., WADE, T., Fusion Technol. **11** (1987) 203.
[34] ZAVOJSKIJ, E.K., KOVAN, I.A., PATRUSHEV, B.I., et al., Zh. Tekh. Fiz. **31** (1961) 513 (in Russian).
[35] STIX, T.H., PALLADINO, R.W., Phys. Fluids **3** (1960) 641.
[36] HOOK, W.M., TENNEY, F.H., BRENNAN, M.H., HILL, H.M., STIX, T.H., Phys. Fluids **4** (1961) 1131.
[37] SHVETS, O.M., KALINICHENKO, S.S., TARASENKO, V.F., PAVLICHENKO, O.S., TOLOK, V.T., Zh. Tekh. Fiz. **35** (1965) 2185 (in Russian).
[38] NAZAROV, N.I., ERMAKOV, A.I., TOLOK, V.T., Zh. Tekh. Fiz. **36** (1966) 612 (in Russian).
[39] WATARI, T., HATORI, T., KUMAZAWA, R., et al., Phys. Fluids **21** (1978) 2076.
[40] OVCHINNIKOV, S.S., KALINICHENKO, S.S., KURILKO, P.I., et al., in Plasma Physics and Controlled Nuclear Fusion Research 1971 (Proc. 4th Int. Conf. Madison, 1971), Vol. 3, IAEA, Vienna (1971) 597.
[41] CARTER, M.D., LYSOJVAN, A.I., MOISEENKO, V.E., et al., Nucl. Fusion **30** (1990) 723.
[42] MOISEENKO, V.E., Fiz. Plazmy **6** (1980) 1174 (in Russian).
[43] SHVETS, O.M., KALINICHENKO, S.S., LYSOJVAN, A.I., et al., Pis'ma Zh. Ehksp. Teor. Fiz. **34** (1981) 533 (in Russian).
[44] KORZH, A.F., STEPANOV, K.N., Fiz. Plazmy **13** (1987) 291 (in Russian); Sov. J. Plasma Phys. **13** (1987) 164.
[45] PARAIL, V.V., PEREVERZEV, G.V., VOJTSEKHOVICH, I.A., in Plasma Physics and Controlled Nuclear Fusion Research 1984 (Proc. 10th Int. Conf. London, 1984), Vol. 1, IAEA, Vienna (1985) 605.
[46] ZAKHAROV, L.E., PEREVERZEV, G.V., Fiz. Plazmy **14** (1988) 141 (in Russian); Sov. J. Plasma Phys. **14** (1988) 75.
[47] PEREVERZEV, G.V., in Plasma Physics and Controlled Nuclear Fusion Research 1988 (Proc. 12th Int. Conf. Nice, 1988), Vol. 1, IAEA, Vienna (1989) 739.

[48] CARTER, M.D., in Stellarator Physics (Proc. 7th Int. Workshop Oak Ridge, TN, 1989), IAEA-TECDOC-558, IAEA, Vienna (1990) 275.
[49] MOISEENKO, V.E., in Problems in Atomic Science and Techniques, Series Thermonuclear Fusion, No. 3, I.V. Kurchatov Inst. Atomic Energy, Moscow (1985) 18 (in Russian).
[50] VACLAVIK, J., APPERT, K., Nucl. Fusion **31** (1991) 1945.
[51] MOISEENKO, V.E., Fiz. Plazmy **12** (1986) 1376 (in Russian); Sov. J. Plasma Phys. **12** (1986) 798.
[52] DOLGOPOLOV, V.V., KRYUKOV, A.V., ROMANOV, S.S., Phys. Fluids **31** (1988) 1649.
[53] MOISEENKO, V.E., in Stellarator Physics (Proc. 8th Int. Workshop Khar'kov, 1991), IAEA, Vienna (1991) 207.

(Manuscript received 15 August 1991
Final manuscript received 21 April 1992)